Does the study of nano-microzooplankton community size structure effectively define their dynamics ? Investigation in the Bay of Biscay (France).

E Marquis, Nathalie Niquil, Christine Dupuy

OXFORD UNIVERSITY PRESS Journal of Plankton Research

Does the study of nano-microzooplankton community size structure effectively define their dynamics ? Investigation in the Bay of Biscay (France).

Journal:	*Journal of Plankton Research*
Manuscript ID:	Draft
Manuscript Type:	Original Article
Date Submitted by the Author:	n/a
Complete List of Authors:	Marquis, Elise; National Taiwan University, Institute of Oceanography Niquil, Nathalie; Université de La Rochelle, UMR 6250, Laboratoire LIENSs Dupuy, Christine; Université de La Rochelle, UMR 6250, Laboratoire LIENSs
Keywords:	nano-microzooplankton, size structure, dynamics, taxonomy, Bay of Biscay

Does the study of nano-microzooplankton community size structure effectively define their dynamics ? Investigation in the Bay of Biscay (France).

Elise MARQUIS *

Laboratoire LIENSs, UMR 6250, Université de La Rochelle, Bâtiment ILE, 2 rue Olympe de Gouges, 17000 La Rochelle, France
E-mail address : emarquis@me.com

Present address : Institute of Oceanography, National Taiwan University, No. 1, Section 4, Roosevelt Road, Taipei, 10617, Taiwan
Tel: 00886(0)983341751
Fax: 00886(0)233669746

Nathalie NIQUIL

Laboratoire LIENSs, UMR 6250, Université de La Rochelle, Bâtiment ILE, 2 rue Olympe de Gouges, 17000 La Rochelle, France
E-mail address : nniquil@univ-lr.fr

Christine DUPUY

Laboratoire LIENSs, UMR 6250, Université de La Rochelle, Bâtiment ILE, 2 rue Olympe de Gouges, 17000 La Rochelle, France
E-mail address : cdupuy@univ-lr.fr

* Corresponding author

ABSTRACT

Studies of nano-microzooplankton dynamics based on the analysis of community taxonomic composition are highly time consuming and manpower demanding. Recent developments in automatic plankton counting technology are offering a new way to consider plankton dynamics with straightforward analysis of community size structures. The present study aimed to ensure that size is a good descriptor of nano-microzooplankton dynamics. The dynamics of the nano-microzooplankton community of the Bay of Biscay (France) over three sites and four sampling periods was analyzed using three different parameters of classification: taxon, body size (ngC $cell^{-1}$) and equivalent spherical diameter (µm). A Mantel test revealed that there was no difference in the characteristics of nano-microzooplankton dynamics when studying either community size structure or taxonomic composition. Moreover, a BEST test confirmed that the biotic and abiotic factors selected for impacting nano-microzooplankton community dynamics were the same among the three classification types. Considering those results, it was argued that nano-microplankton dynamics is well defined by the study of the community size structure. While focusing on nano-microzooplankton size structure seems promising, homogenizing the size descriptor used among studies would be needed in order to make worldwide data comparisons and ESD/biovolume should be favored.

KEYWORDS: nano-microzooplankton, size structure, dynamics, taxonomy, Bay of Biscay

INTRODUCTION

Open ocean photosynthesis is dominated by pico-nanophytoplanktonic production (0.2 to 20 m diameter, Sieburth et al., 1978), with most of the active primary producers smaller than 3 μm (Waterbury et al., 1979; Fenchel, 1988). A complex assemblage of viruses, bacterioplankton and protozoans coexist with and support these small oceanic primary producers through their role in nutrient regeneration (Azam et al., 1983; Ducklow and Carlson, 1992; Sherr and Sherr, 2000). Larger phytoplankton such as diatoms and dinoflagellates show greater variability than pico-nanophytoplankton and so do their predators, i.e. larger protists and metazoans (Fenchel, 1988). Primary production is transferred to higher levels through two main pathways: classical food chain and microbial food web, according to the size of the main primary producers (Azam et al., 1983; Sherr et al., 1986; Sommaruga, 1995; Thingstad and Rassoulzadegan, 1999). Therefore, depending on which pathways is dominating the planktonic food web, the amount of energy lost (mainly through respiration), matter recycled and organic carbon available to plankton predators (mainly fish) will vary. For those reasons, our understanding of plankton dynamics and plankton food web functioning is intimately related to our appreciation of global biogeochemical fluxes. Despite the actual need for information about these issues when studying global warming concerns, the current amount of knowledge of the identity and the functional role of the major plankton groups as well as their dynamics prevent us evolving from the current simple plankton models towards more detailed and adaptative ecosystem modeling (Ducklow, 2003).

Since the paper of Azam et al. (1983), a high number of studies have focused on the dynamics and the role of nano-microzooplankton in oceanic, coastal and halieutic environments. Nano-microzooplankton are trophic intermediaries in pelagic food webs, permitting the transfer of carbon from pico- and nanoplankton to the metazoans (Sherr et al., 1986; Pierce and Turner, 1992). They occupy an essential trophic node in microbial food webs and their dynamics may be either controlled by predation or by resource availability as well as hydrography (e.g. Sanders, 1987; Cowlishaw, 2004). Despite such an essential role in the aquatic ecosystems, their taxonomical diversity is so high that it is clear that they are not perfectly known. In the early nineties, Sleigh (1991) discussed about the taxonomy of heterotroph protists, which are the main components of the nano-microzooplankton community, and stated “many species, and possibly phyla, remain to be described” (Sleigh, 1991). Today, almost twenty years later, and despite progress in DNA sequencing, protozoan taxonomy is still subject to study, discussion and controversy (e.g. Finlay, 2004; Adl et al., 2005).

Traditional studies based on taxonomic compositions of plankton communities are difficult to implement efficiently due to the limitation of resources, time and manpower to process samples

(Culverhouse et al., 2006). However, size is another possible way to classify plankton organisms, and the terminology of Sieburth (Sieburth et al., 1978) is useful and has become widely accepted. Recent development in metabolic theory (Brown et al., 2004) confirms older studies (e.g. Moloney and Field, 1989) on suggesting that size determines many biological properties of organisms such as respiration, nutrient uptake, production, ontogenetic growth, etc…(e.g. Zeuthen, 1970; Gillooly et al., 2001; West et al., 2003; Lupez-Urrutia et al., 2006). Moreover, in aquatic ecosystems, size usually determines predator-prey interactions (e.g. Frost, 1972; Peters and Downing, 1984; Caparroy et al., 2000). As such, size distribution of plankton may be used as indicators of ecosystem and trophic status. Additionally, recent studies have shown that one of the aquatic ecological responses to global warming is the reduction of body size (Daufresne et al., 2009; Moran et al., 2010). Regarding all these issues, studying planktonic and especially nano-microzooplanktonic dynamics based on the community size structure seems to be an interesting and promising research focus.

New technologies for automatic plankton counting are now available to plankton ecologists. Such instruments, e.g. the Flowcam technology (Sieracki et al., 1998), are excelling in size classification and identification of planktonic cells. Therefore, they would be very useful in studying the dynamics of planktonic community size structures. However, before commencing such studies, it is essential to ensure that size is a sufficient plankton community descriptor on its own. In other words, it is essential to understand if the dynamics resulting from those size-based analyses are showing the same pattern and the same spatio-temporal differences as the dynamics resulting from the taxonomy-based analysis.

This study aims to investigate whether the seasonal and spatial dynamics of the nano-microzooplankton may be revealed looking at the size structure of the community. Extensive data on planktonic communities collected in 2004 in the Bay of Biscay were used to answer this question. Size-Abundance spectra are used to understand the overall changes in the nano-microzooplankton composition and a comparison between taxon-based and size-based classifications helps to evaluate the relevance of the size structure analysis.

MATERIAL AND METHODS

Study site and hydrography

The continental shelf of the Bay of Biscay (Fig. 1) is up to 200 km wide with a surface area of 223,000 km². Its hydrological structure is principally influenced by the seasonal dynamics of the

Loire and the Gironde river plumes (Lazure and Jegou, 1998) and the shelf ecology shows a strong variability in time related to temperate zone climatic fluctuations (Koutsikopoulos et al., 1998). At four periods in 2004 (08 to 10 February, 23 to 25 April, 09 to 11 June, and 30 September to 02 October), three stations were sampled, located on the continental shelf, on an estuary-coast-offshore triangle: "Gironde" (01°30W, 45°30N), "Coast" (01°30W, 45°01N) and "Offshore" (2°20W, 45°10N) (Fig. 1). Salinity and temperature profiles were measured using a CTD (Conductivity-Temperature-Density) probe (Sea-Bird SBE 9). Concurrently, irradiance and fluorescence profiles of the water column were measured in order to measure the depths of the photic zone and maximum fluorescence in order to adapt the plankton sampling accordingly.

Water and plankton sampling and analysis

At each station and sampling period, we collected water samples with 12-L Niskin bottles at three different depths: subsurface, maximum fluorescence and bottom of the photic zone.

Samples for dissolved inorganic nutrients analyses: nitrate (NO_3), nitrite (NO_2), silicate ($Si(OH)_4$) and phosphate (PO_4), were immediately filtered through Whatman GF/F filters so that the filtrate could be stored at - 20°C until its analysis at the laboratory with a Skalar autoanalyzer (Strickland and Parsons, 1972).

Samples for bacteria and picophytoplankton counting were fixed with formaldehyde (final concentration 2%), frozen in liquid N_2 and enumerated using a FACSCan flow cytometer (Bd-Bioscience) (Marie et al., 2000). Nanoflagellates were fixed with buffered paraformaldehyde (final concentration 1%) then stained with DAPI and counted on 0.8 µm black polycarbonate filters by epifluorescence microscopy (Sherr et al., 1994). Heterotrophic nanoflagellates (HNF) were distinguished from pigmented (autotrophic) nanoflagellates (ANF) by the absence of chlorophyll fluorescence. Microphytoplankton (diatoms and dinoflagellates) were fixed with formaldehyde (final concentration 1%) plus alkaline lugol (final concentration 1%), enumerated and measured by inverse microscopy (Utermöhl, 1958). Heterotrophic and mixotrophic dinoflagellates (HDF) were determined from morphologic species recognition and relevant literature (e.g. Lessard and Swift, 1986). Ciliates were stained with alkaline lugol (1% final concentration), counted and measured by inverse fluorescence microscopy. Ciliate samples from surface and bottom of the photic zone collected in February at the Gironde station were not analyzed due to poor preservation. Diatom, dinoflagellate and ciliate biovolumes were calculating by transforming the cell's shapes into geometric figures. Samples of metazoan microplankton were obtained by gently filtering 10 liters of collected seawater through a 63µm size mesh. The retained organisms were then diluted in

filtered (< 63 µm) seawater and preserved in buffered formaldehyde (final concentration 2%). They were counted under a binocular microscope. All the conversion factors and equations used to convert the abundance of pico-, nano- and microplankton into biomass were obtained from the literature (Table 1). The equivalent spherical diameter (ESD) of each cell was obtained by calculating the diameter (µm) of a hypothetical sphere of equivalent volume. The two conversion from biovolume to biomass and from biovolume to ESD resulted in an exponential relationships between the body mass and ESD of nano-microzooplankton cells in this study (Figure 2).

Mesozooplankton was collected from vertical tows through the entire photic zone using a 200µm-mesh WP2 net, preserved in buffered formaldehyde (final concentration 2%) and counted under a binocular microscope. A second replicate was used to measure the mesozooplankton dry weight. Mesozooplankton carbon biomass was determined by multiplying dry weights of each sample by a factor of 0.38 (Bode et al., 1998).

Data analysis

Size-abundance spectra (SAS) were obtained by presenting the $\log_{10}$ of the abundances (cells mL^{-1}) versus the $\log_{10}$ of the geometric mean of the respective size class (μm^3).

The nano-microzooplankton community was then classified under 3 different classification types:

1- Taxons: Heterotrophic nanoflagellates (HNF); Unarmoured Heterotrophic dinoflagellates (U-HDF); Armoured Heterotrophic dinoflagellates (A-HDF); Naked Ciliates; Tintinnid Ciliates; *Myrionecta rubra* ciliates; Microplanktonic metazoans.

2- Body Sizes: <100 ngC $cell^{-1}$; 100 to 1,000 ngC $cell^{-1}$; 1,000 to 5,000 ngC $cell^{-1}$; 5,000 to 10,000 ngC $cell^{-1}$; 10,000 to 50,000 ngC $cell^{-1}$; 50,000 to 100,000 ngC $cell^{-1}$; >100,000 ngC $cell^{-1}$.

3- ESD (Equivalent Spherical Diameter): <20 µm; 20 to 30 µm; 30 to 40 µm; 40 to 50 µm; 50 to 60 µm; 60 to 70 µm; >70 µm.

All data were normalized prior to statistical analyses; using a double-root-transformation on the abundance and biomass data and a log-transformation on the environmental data (Legendre and Legendre, 1998). Two types of analyses were applied to the data sets: Mantel test (Legendre and Legendre, 1998) to analyze whether the different ways of classifying nano-microzooplankton lead to different description of its spatial/temporal dynamics, and BEST test, to analyze the biotic (i.e. trophic) and abiotic (i.e. environmental) factors impacting nano-microzooplankton community dynamics and to compare the factors selected for each classification types.

First, we constructed 3 matrices using nano-microzooplankton abundances of the 3 classification types (Taxons, Body Sizes and ESD). We used the average abundance values throughout the water column. The 3 matrices have 12 rows (3 sites and 4 sampling periods) and 7 columns (7 different classes, for each classification). These matrices were used to calculate dissimilarity matrices in order to model the resemblance between the sampled sites/months by the mean values of community composition for each of the 3 nano-microzooplankton classification types. Bray and Curtis distance measure was used because it's particularly suitable for quantitative data (Legendre and Legendre, 1998). We then applied the Mantel test to see if there was a correlation between the different distances matrices (Legendre and Legendre, 1998). In a simple Mantel test, two matrices were compared. First a Pearson correlation (r) was calculated between the matrices and after this, the second matrix was shuffled 10,000 times and the correlation recalculated. This permutation procedure was done in order to construct a law of distribution of correlation coefficients, in absence of statistically significant relation between the two matrices. The original coefficient was then compared with this distribution in order to determine its statistical significance (p value). The Mantel statistics were calculated for the 3 pairs formed by the different nano-microzooplankton classifications: Taxons/Body Sizes, Taxons/ESD, Body Sizes/ESD.

The second analysis was a BEST test (Clarke and Warwick, 2001) done using the software package PRIMER®6. The BEST analysis selected trophic and environmental variables that best explain patterns in the nano-microzooplankton assemblage. The test was conducted by maximizing a Spearman rank correlation between the resemblance matrices of environmental and trophic variables (Euclidean distance) and community abundances (Bray-Curtis distance). The significance of these results was tested using permutation tests. The environmental parameters analysed were: Temperature (°C), Salinity (PSU), NO_2 concentration (µmol l^{-1}), $N0_3$ concentration (µmol l^{-1}), PO_4 concentration (µmol l^{-1}) and N/P ratio. The trophic parameters tested were the biomasses (µgC l^{-1}) of the possible nano-microzooplankton's preys as well as their possible predators: Heterotrophic Bacteria, Cyanobacteria, Picoeukaryotes, Autotrophic Nanoflagellates, Autotrophic Dinoflagellates <20 µm, Autotrophic Dinoflagellates >20 µm, Diatoms <20 µm, Diatoms >20 µm, and Mesozooplankton.

RESULTS

Seasonal and spatial dynamics of environmental conditions.

At the Gironde and Coast sites (Fig. 3), the water column varied from halostratified in winter and spring to thermostratified in summer. In June at these two coastal sites, the water column showed both types of stratification (Fig. 3). For example, at the Gironde site, changes in salinity and temperature between the surface to a depth of 10 meters were 31.8 PSU to 34.3 PSU, and 17.2°C to 14.7°C, At the Offshore site, the water column showed a moderate halostratification in June with only a surface salinity of 34.5 PSU (Fig. 3). The water column at the Offshore site was not stratified in winter and early spring (February and April, Fig. 3) but became progressively thermostratified from June to October; in late summer the water's temperature stays around 20.1°C from the surface to a depth of 30 m subsequently dropping lower than 18°C below a depth of 40 m (Fig. 3).

At the three sites, the highest average concentrations of total NO (NO_2 and NO_3) along the photic zone were observed in February with, for example, 12.1 ± 1.6 µmol l^{-1} at the Gironde site (Fig. 4). In April, June and September, NO average concentrations varied from 5.8 ± 0.6 to 0.2 ± 0.1 µmol l^{-1} along the photic zones of the 3 studied sites (Fig. 4). Considering all three sites and all 4 studied periods, the average $Si(OH)_4$ concentrations along the photic zone were always lower than 6 µmol l^{-1} and the average PO_4 concentrations along the photic zone never exceeded 1 µmol l^{-1} (Fig. 4). The N/P ratio was highest in April at the two coastal sites (77 at Gironde and 173 at Coast) and lowest in September (below the Redfield ratio with 10 at Gironde and 11 at Coast). The highest N/P ratio at Offshore site was found in September but didn't exceed 13.

Seasonal and spatial variations in phytoplankton biomass and composition

The average autotrophic biomass along the photic zone decreased from February to October at the Gironde site (376.6 ± 459.3 µgC l^{-1} to 10.9 ± 2.4 µgC l^{-1}, Fig. 5). At the Coast and Offshore sites, the average autotrophic biomass along the photic zone first increased between February and April, reaching, respectively, 116.2 ± 15.6 µgC l^{-1} and 155.8 ± 40.1 µgC l^{-1} (Fig. 5a) and then decreased in June and October. Large diatoms were responsible for more than 70% of the total biomass in February, April and June at the Gironde site and in February and April at both Coast and Offshore sites (Fig. 5b). In February, diatoms were dominated by large chain forming cells (e.g. *Thalassiosira sp.*) at the two coastal sites. Smaller diatoms (i.e. diatoms <20 µm) such as *Leptocylindrus minumus* became more abundant in April at Coast site (Fig. 5b). The biomass of smaller autotrophs (ANF, cyanobacteria and picoeukaryotes) proportionally increased from April to October at all three stations and dominated in October (> 60% of average biomass, Fig. 5b).

Seasonal and spatial variations of nano-microzooplankton biomass and taxonomic composition

At the three sites, average biomasses along the photic zone of nano-microzooplankton peaked in April at Gironde, Coast and Offshore with 27.9 ± 13.2 µgC l^{-1}, 57.1 ± 32.8 µgC l^{-1} and

27.2 ± 13.6 µgC l^{-1}, respectively (Fig. 6a). The average biomass was still relatively high in June at the Gironde and Coast sites (> 19.5 µgC l^{-1}, Fig. 6a) but never exceeded 8.2 µgC l^{-1} in February and October. The Offshore site always had the lowest average biomasses of the three sites (Fig. 6a).

Ciliates, especially naked ciliates, counted for a large part (> 70%, Fig. 6b) of the total average nano-microzooplankton biomass at Coast site in February and April as well as in April at Offshore site. The relative proportion of ciliates in the average biomass of nano-microzooplankton was always the highest in April at the three studied sites (Fig 6b). The relative proportion of nauplii biomass was higher in February and October compare to April and June at all sites (Fig. 6b) despite small range of variations of their absolute abundances. The rest of the nano-microzooplankton biomass was largely due to the unarmoured dinoflagellates (up to 61.8% of the total biomass, in June at Offshore site, Fig. 6b). Even though the HNF had very high abundances (Table 2), their contribution to the total biomass of the nano-microzooplankton was very low, overall less than 8% (Fig. 6b).

Seasonal and spatial dynamics of nano-microzooplankton size structure.

Analysis of the size-abundance spectra (SAS) showed typical linear relationships at every sites and every sampling period with regression coefficients comprised between 0.7 and 0.9 (Fig. 7). Linear regression slope of the SAS at the Offshore site presented the highest temporal variations with a decrease from -1.02 in February to -0.68 in April (Fig. 8). Both SAS slopes at the Offshore and Coast sites decreased from February to April and then increased from April to October (Fig. 8). At the Gironde site, the SAS slope varied slightly along the first three sampling periods but its value increased in October and became very similar to the slopes of the two other sites (-0.85, -0.87 and -0.89 respectively at Gironde, Coast and Offshore sites; Fig. 8).

Despite large variations in their abundances (Table 2), the relative proportion of most of the small ESD size classes to the total biomass did not vary remarkably and remained low during the 4 sampling periods (Fig. 9a). Cells measuring less than 40 µm ESD never counted for more than 16% of the total nano-microzooplankton biomass at any of the sites (Fig. 9a). The relative proportion of the 40-50µm ESD-size class was at all times much higher with values above 16% (Fig. 9a). Furthermore, it dominated the community in June at Gironde and Coast sites, contributing for 72.1% and 68.2% of the total biomass, respectively, (Fig. 9a) with cell abundances of several thousand per liter (Table 2). With the exception of April, the nano-microzooplankton biomass at Offshore site was always dominated by this 40-50 µm ESD-size class with a relative proportion greater than 40% (Fig. 9a). Large microzooplankton (> 60µm ESD) contributing substantially to the total community biomass in February and October at Gironde and Coast, with a relative proportion greater than 46% and in April at Offshore site with a relative proportion of 52.8% (Fig. 9a).

The dynamics of the nano-microzooplankton body size structure followed the same pattern as the ESD size structure (Fig. 9b). The small body size classes (< 1 ngC $cell^{-1}$) didn't contribute significantly to the final community biomass (<24.5%, Fig. 9b) but had very high abundance (Table 2). The relative proportion of the intermediate body size class (1-5 ngC $cell^{-1}$) was the highest in June at the three sites and this size class dominated the final community biomass in April and June at Gironde, in June at Coast and in February and June at Offshore (Fig. 9b). The largest body size classes (>10 ngC $cell^{-1}$) dominated the nano-microzooplankton biomass in February and October at Gironde and Coast sites and in April at Coast and Offshore sites (Fig. 9b) but never dominated the total community abundance (Table 2).

Comparing the three classification types.

The Mantel test revealed a positive and significant correlation between the three microzooplankton classification types (Table 3). The level of similarities between each of the 12 data sets (3 sites and 4 sampling periods) in terms of nano-microzooplankton composition was comparable with every classification we used ($r > 0.8$ and $p < 0.0001$). In other words, there was no difference in the characteristics of nano-microzooplankton dynamics when studying either community size structure or taxonomic composition.

Linking nano-microzooplankton dynamics and environmental conditions.

Rank correlation of physical variables to the nano-microzooplankton abundances indicated that the best physical variables driving community patterns were temperature and NO_3 concentration whatever classification types we were using (Table 4). BEST analysis also showed that the nano-microzooplankton dynamic was associated with bacterial and cyanobacterial dynamics with every classification types were used. These associations were also observed with ANF dynamics when using ESD and Taxons classifications only (Table 4). It was finally noted that the correlation coefficient obtained with the BEST analyses, while significant, were not in any case very high (< 0.5, Table 4).

DISCUSSION

In temperate marine environments, seasonal variations of the physico-chemical parameters of the water column have a strong influence on the structure of phytoplanktonic communities (Margalef, 1958; Fenchel, 1988; Breton et al., 2000; Chang et al., 2003). In summer, vertical stratification is generally associated with nutrient limitation and regenerated production based on the uptake of ammonium by small-celled phytoplankton populations (Margalef, 1958; Valiela, 1995; Chang et al., 2003). On the other hand, winter/spring vertical mixing is usually associated

with nitrate availability and new production by large-celled phytoplankton populations (Margalef, 1958; Valiela, 1995; Bury et al., 2001; Irigoien et al., 2005). In addition, coastal areas receiving river runoffs may see that latter increased due to the accumulation of terrestrial nutrients in late winter/spring (Domingues et al., 2005; Alvarez et al., 2009). Although the Bay of Biscay makes no exception with highest thermostratification of the water column in late summer at the three studied sites and high concentrations of nitrate in late winter at the site closest to the Gironde estuary, areas under the influence of the Gironde runoff showed high halostratification of the water column as soon as February. As a consequence, phytoplankton biomass and composition present strong spatio-temporal variations with large diatoms dominating the community in winter/spring and small autotrophic cells dominating in late summer. Nano-microzooplankton is a direct predator of phytoplankton cells (Capriulo, 1991; Capriulo et al., 1991; Calbet and Landry, 2004). As a bottom-up effect, we can assume that changes in nano-microzooplankton community will follow changes in phytoplankton community structure. Indeed, heterotrophic protist abundances have been described as a function of food availability in many previous studies (e.g. Dolan and Coats, 1990). Following this argument, the lack of suitable resources in September (dominance of cyanobacteria) and February (large diatoms) might be the principal factor responsible for the low summer and winter nano-microzooplankton biomasses in the Bay of Biscay. Verity (1986) and Lynn and Montagnes (1991) show that the distribution of ciliates generally present a close association with nanophytoplankton in temperate coastal ecosystems. In this study, ciliate biomasses seem more closely related to microphytoplankton than nanophytoplankton but this might be because those kinds of biomass composition snapshots are not powerful in showing the real level of produced biomass of highly grazed prey. However, the BEST analysis revealed that ANF biomasses were one of the main factors explaining the changes in the nano-microzooplankton taxonomic structure. In late summer, the proportion of nauplii in the nano-microzooplankton community increases along the coast of the Bay of Biscay since most of the reproduction of adult copepods occurs during summer (Sautour and Castel, 1998).

Most of the trophic relationships within planktonic food webs are based on size, i.e. the larger consuming the smaller (Platt and Denman, 1977; Moloney and Field, 1991; Caparroy et al., 2000; Stock et al., 2008). Therefore, the size structure of nano-microzooplankton should reflect the phytoplanktonic composition with large grazers more abundant when large diatoms are the main primary producers. When the community is described with SAS, this situation would then correspond to flatter slopes, i.e. lower absolute values (Platt and Denman, 1977; Rodriguez and Mullin, 1986). This is what was observed with this data. The slopes of the linear regression, when fitted to the SAS, are steepest (i.e. highest absolute value) in October when bacteria are very abundant and when picophytoplankton is the principal primary producer. The three study sites show

time differences in the phytoplanktonic dynamics with a diatom bloom occurring as soon as February at Gironde but only in April at Coast and Offshore. This difference is visible when analyzing the nano-microzooplankton SAS slope changes at the three sampling sites. The estuarine site, Gironde, has a flatter slope in February due to the presence of bigger cells in the nano-microzooplankton community. The SAS slopes at Coast and Offshore decrease in April showing an increase of large cells in the nano-microzooplankton when the bloom of diatoms is peaking at those two sites.

In the literature, most of the studies on plankton size structure are focused on phytoplankton (e.g. Cermeno and Figueiras, 2008) or the modeling of the whole planktonic community (e.g. Baird and Suthers, 2007). However, with the increasing interest on nano-microzooplankton community as a major player of the planktonic food web (Azam et al., 1983), numerous studies are describing the nano-microzooplankton dynamics in very different environments (e.g. Shinada et al., 2003; Gaedke and Wickham, 2004; Fileman and Leakey, 2005). Identification of nano-microzooplankton cells through classical microscopic methods is highly time consuming and new technologies such as automatic plankton counters are quickly extending their attraction among ecologists (see review in Benfield et al., 2007). But those technologies, despite being very efficient at counting cells, do not have the same capabilities in cell identification as an expert human eye. A good understanding of the community dynamics depends on a good description of its composition and structure. Size parameters of nano-microzooplankton cells are easy to compile but the question is whether it is a sufficient descriptor on its own.

The first problem occurs when choosing the best size parameter to use. Each study corresponds to a different parameter: length, diameter, equivalent spherical diameter, biovolume, cell carbon content, etc…(e.g. Kimmel et al., 2006; Cermeno and Figueiras, 2008; Basedow et al., 2009). Despite the will to describe the same characteristic of a cell and its size, this variety may be an obstacle to those who would like to compare data from different studies. In this study, the three most widely used parameters where purposely used: biovolume, ESD and body mass. Since ESD and biovolume are directly related to one another, one can be used to compare the structure of the other without any difficulties. But depending on the conversion factor used, the body mass may not be directly proportional to the first two parameters. In this case, the general relationship between ESD and body mass matches an exponential slope. Although ESD is not representing the trophic value of the nano-microzooplanktonic cell, it is an easier parameter to measure or estimate than the body mass. Moreover, since the definition of ESD is the same for cells of every size and every sea, it would be more reliable as a comparable and universal parameter. Therefore, we recommend on using ESD as a proxy of size when studying nano-microzooplanktonic size structure.

The second problem, and without doubt the most important, concerns the efficiency of size descriptors to define nano-microzooplankton dynamics as clearly as the taxonomy. Before answering that problem, the definition of "dynamics" of community needs to be agreed upon. As proposed in Lindeman's paper on tropho-dynamics (1942), the dynamics of a community is the pattern of its changes in size and composition over time and space resulting from the coactions between the living members of the community and reactions of those members with the non-living environment. Following that definition, the nano-microzooplankton dynamics portrayed with size descriptors should show the same pattern of changes and of differences between seasons and sites as the dynamics portrayed with taxonomy. The Mantel test used in this study focused on comparing the patterns of the spatio-temporal differences observed in the size and composition of the nano-microplankton community with three different descriptors (taxonomy and two size parameters). Statistics didn't divulge any differences between the three dynamics. Therefore, we can argue that using the size structure to characterize the dynamics of nano-microplankton lead to revealing the same spatio-temporal patterns when using a taxonomic structure.

Finally, the ultimate goal of community dynamics studies is the understanding of the relationships of a community with its environment and more precisely with its trophic environment (i.e. Lindeman, 1942). Knowledge of community dynamics is necessary in food webs and ecosystem process studies as it provides a way to analyze the transfer rates of energy matter and the impact of environmental disturbances (de Ruiter et al., 2005). The historical way to examine community dynamics was by changes in its taxonomic structure and the trophic relationships between taxonomical groups (e.g. Andersen and Sorensen, 1986; Uitto et al., 1997). We have shown with this study that size descriptors were efficiently defining nano-microzooplankton dynamics, but are they also good in revealing biotic and abiotic factors controlling that dynamics? Although correlations do not necessary mean direct causal relationships such as trophic links, they might give information on the physical and biological parameters influencing the nano-microzooplankton dynamics (Legendre and Legendre, 1998). In our study, the interest of such an analysis was to compare the results obtained with the three different types of classification. The results of the BEST analyses were the same for the three types of classification compared in our study with very low but similar Spearman rank correlation coefficients. The only difference was found with the Body size classification, for which only two biological parameters were significantly explaining the nano-microzooplanktonic dynamics, compared to the three found for the two other classifications.

In conclusion, considering the results of our study, we argue that nano-microplankton dynamics are well defined by the study of their size structure. The use of automatic plankton counters such as the Flowcam technology (Sieracki et al., 1998) is therefore relevant despite the

lack of precise taxonomical identification. However, homogenizing the size descriptor used among studies is needed in order to make worldwide data comparisons and ESD/biovolume should be favored. We also recommend further investigations on size-based trophic relationships and size structure dynamics in order to confirm the results found in the Bay of Biscay.

ACKNOWLEDGEMENTS

This study was supported by the French "Programme National Environment Côtier" – Bay of Biscay working site – and Ifremer. The authors wish to thank captains and crews of R/V Thalia for support activities, C. Courties (Observatoire Océanologique de Banyuls, France) for the flowcytometry analyses, F. Mornet (IFREMER, FREDD, France) and V. Huet (LIENSs, France) for nutrient and chlorophyll measurements, P. Malterre and M-J Capdeville (students of University of La Rochelle, France) for metazoan counts.

BIBLIOGRAPHY

Adl S.M., Simpson, A.G.B., Farmer, M.A., Andersen, R.A., Anderson, O.R., Barta, J.R., Bowser, S.S., Brugerolle, G., Fensome, R.A., Fredericq, S., James, T.Y., Karpov, S., Kugrens, P., Krug, J., Lane, C.E., Lewis, L.A., Lodge, J., Lynn, D.H., Mann, D.G., Mccourt, R.M., Mendoza, L., Moestrup, O., Mozley-Standridge, S.E., Nerad, T.A., Shearer, C.A., Smirnov, A.V., Spiegel, F.W., Taylor, M.F.J.R. (2005) The new higher level classification of eukaryotes with emphasis on the taxonomy of protists. *Journal of Eurkaryotic Microbiology,* **52**, 399-451

Alvarez E., Nogueira, E., Acuna, J.L., Lopez-Alvarez, M., Sostres, J.A. (2009) Short-term dynamics of late-winter phytoplankton blooms in a temperate ecosystem (Central Cantabrian Sea, Southern Bay of Biscay). *J Plankton Res,* **31**, 601-617

Andersen P., Sorensen, H.M. (1986) Population dynamics and trophic coupling in pelagic microorganisms in eutrophic coastal waters. *Mar Ecol Prog Ser,* **33**, 99-109

Azam F., Fenchel, T., Field, J.G., Gray, J.S., Meyer-Reil, L.A., Thingstad, F. (1983) The ecological role of water-column microbes in the sea. *Mar Ecol Prog Ser,* **10**, 257-263

Baird M.E., Suthers, I.M. (2007) A size-resolved pelagic ecosystem model. *Ecol Model,* **203**, 185-203

Basedow S.L., Tande, K.S., Zhou, M. (2009) Biovolume spectrum theories applied: spatial patterns of trophic levels within a mesozooplankton community at the polar front. *J Plankton Res*, fbp110

Benfield M.C., Grosjean, P., Culverhouse, P., Irigoien, X., Sieracki, M.E., Lopez-Urrutia, A., Dam, H.G., Hu, H.G., Davis, Q., Hansen, A., Pilskaln, C.H., Riseman, E., Schultz, H., Utgoff, P.E., Gorsky, G. (2007) RAPID - Research on Automated Plankton Identification. *Oceanography,* **20**, 12-26

Blanchot J., Rodier, M. (1996) Picophytoplankton abundance and biomass in the western tropical Pacific Ocean during the 1992 El Nino year: results from flow cytometry. *Deep-Sea Res Pt I,* **43**, 877-895

Bode A., Alvarez-Ossorio, M., Gonzalez, N. (1998) Estimation of mesozooplankton biomass in a coastal upwelling area off NW Spain. *J Plankton Res,* **20**, 1005-1014

Breton E., Brunet, C., Sautour, B., Brylinski, J.-M. (2000) Annual variations of phytoplankton biomass in the Eastern English Channel: comparison by pigment signatures and microscopic counts. *J Plankton Res,* **22**, 1423-1440

Brown J.H., Gillooly, J.F., Allen, A.P., Savage, V.M., West, G.B. (2004) Toward a metabolic theory of ecology *Ecology,* **85**, 1771-1789

Bury S.J., Boyd, P.W., Preston, T., Savidge, G., Owens, N.J.P. (2001) Size-fractionated primary production and nitrogen uptake during a North Atlantic phytoplankton bloom: implications for carbon export estimates. *Deep-Sea Res Pt I,* **48**, 689-720

Calbet A., Landry, M.R. (2004) Phytoplankton growth, microzooplankton grazing, and carbon cycling in marine systems. *Limnol Oceanogr,* **49**, 51-57

Caparroy P., Thygesen, U.H., Visser, A.W. (2000) Modelling the attack success of planktonic predators: patterns and mechanisms of prey size selectivity. *J Plankton Res,* **22**, 1871

Capriulo G.M. (1991) Community grazing in heterotrophic marine protista - session summary. In: Reid P.C., Turley, C.M. and Burkill, P.H. (eds) *Protozoa and their role in marine processes*. Springer-Verlag, Berlin, pp. 205-218

Capriulo G.M., Sherr, E.B., Sherr, B.F. (1991) Trophic behaviour and related community feeding activities of heterotrophic marine protists. In: Reid P.C., Turley, C.M. and Burkill, P.H. (eds) *Protozoa and their role in marine processes*. Springer-Verlag, Berlin, pp. 219-265

Cermeno P., Figueiras, F.G. (2008) Species richness and cell-size distribution: size structure of phytoplankton communities. *Mar Ecol Prog Ser,* **357**, 79-85

Chang F.H., Zeldis, J., Gall, M., Hall, J. (2003) Seasonal and spatial variation of phytoplankton assemblages, biomass and cell size from spring to summer across the north-eastern New Zealand continental shelf. *J Plankton Res,* **25**, 737-758

Clarke K.R., Warwick, R.M. (2001) *Changes in marine communities: an approach to statistical analysis and interpretation (PRIMER-E)*, Plymouth Marine Laboratory, Plymouth, UK

Cowlishaw R.J. (2004) Seasonal coupling between ciliate and phytoplankton standing stocks in the South Slough of Coos Bay, Oregon. *Estuaries,* **27**, 539-550

Culverhouse P., Williams, R., Benfield, M.C., Flood, P.R., Sell, A.F., Mazzocchi, M.G., Buttino, I., Sieracki, M. (2006) Automatic image analysis of plankton: future perspectives. *Mar Ecol Prog Ser,* **312**, 297-309

Daufresne M., Lengfellner, K., Sommer, U. (2009) Global warming benefits the small in aquatic ecosystems. *P Nat Acad Sci USA,* **106**, 12788-12793

de Ruiter P.C., Wolters, V., Moore, J.C. (2005) Dynamic food webs. In: de Ruiter P.C., Wolters, V. and Moore, J.C. (eds) *Dynamic food webs*. Academic Press, pp. 3-9

Dolan J.R., Coats, D.W. (1990) Seasonal abundances of planktonic ciliates and microflagellates in mesohaline Chesapeake Bay Waters. *Est Coast Shelf S,* **31**, 157-175

Domingues R.B., Barbosa, A., Galvao, H. (2005) Nutrients, light and phytoplankton succession in a temperate estuary (the Guadiana, south-western Iberia). *Est Coast Shelf S,* **64**, 249-260

Ducklow H.W. (2003) Biogeochemical Provinces: towards a JGOFS synthesis. In: Fasham M.J.R. (ed) *Ocean Biogeochemistry - The role of the ocean carbon cycle in Global Change*. Springer, Berlin, pp. 3-17

Ducklow H.W., Carlson, C.A. (1992) Oceanic Bacterial Production. *Adv Microb Ecol,* **12**, 113-181

Fenchel T. (1988) Marine plankton food chains. *Annu Rev Ecol Syst,* **19**, 19-38

Fileman E.S., Leakey, R.J.G. (2005) Microzooplankton dynamics during the development of the spring bloom in the north-east Atlantic. *J Mar Biol Ass UK,* **85**, 741-753

Finlay B.J. (2004) Protist taxonomy: an ecological perspective. *Philosophical Transactions of the Royal Society of London. Series B: Biological Sciences,* **359**, 599-610

Frost B.W. (1972) Effects of size and concentration of food particles on the feeding behavior of the marine planktonic copepod Calanus pacificus. *Limnol Oceanogr,* **17**, 805-815

Gaedke U., Wickham, S.A. (2004) Ciliate dynamics in response to changing biotic and abiotic conditions in a large, deep lake (Lake Constance). *Aquat Microb Ecol,* **34**, 247-261

Gillooly J.F., Brown, J.H., West, G.B., Savage, V.M., Charnov, E.L. (2001) Effects of Size and Temperature on Metabolic Rate. *Science,* **293**, 2248-2251

Gowing M.M., Garrison, D.L., Wishner, K.F., Gelfman, C. (2003) Mesopelagic microplankton of the Arabian Sea. *Deep-Sea Res Pt I,* **50**, 1205-1234

Irigoien X., Flynn, K.J., Harris, R.P. (2005) Phytoplankton blooms: a 'loophole' in microzooplankton grazing impact? *J Plankton Res,* **27**, 313-321

Kimmel D.G., Roman, M.R., Zhang, X.S. (2006) Spatial and temporal variability in factors affecting mesozooplankton dynamics in Chesapeake Bay: Evidence from biomass size spectra. *Limnol Oceanogr,* **51**, 131-141

Koutsikopoulos C., Beillois, P., Leroy, C., Taillefer, F. (1998) Temporal trends and spatial structures of the sea surface temperature in the Bay of Biscay. *Oceanol Acta,* **21**, 335-344

Labry C., Herbland, A., Delmas, D. (2002) The role of phosphorus on planktonic production of the Gironde plume waters in the Bay of Biscay. *J Plankton Res,* **24**, 97-117

Lazure P., Jegou, A.-M. (1998) 3D modelling of seasonal evolution of Loire and Gironde plumes on Biscay Bay continental shelf. *Oceanol Acta,* **21**, 165-177

Legendre P., Legendre, L. (1998) *Numerical ecology*, Elsevier, Amsterdam

Lessard E.J., Swift, E. (1986) Dinoflagellates from the North Atlantic classified as phototrophic or heterotrophic by epifluorescence microscopy. *J Plankton Res,* **8**, 1209-1215

Lindeman R.L. (1942) The Trophic-Dynamic Aspect of Ecology. *Ecology,* **23**, 399-417

Lupez-Urrutia Å., San Martin, E., Harris, R.P., Irigoien, X. (2006) Scaling the metabolic balance of the oceans. *P Nat Acad Sci USA,* **103**, 8739-8744

Lynn D.H., Montagnes, D.J.S. (1991) Global production of heterotrophic marine planktonic ciliates. In: Reid P.C., Turley, C.M. and Burkill, P.H. (eds) *Protozoa and their role in marine processes*. Springer-Verlag, Berlin, pp. 281-307

Margalef R. (1958) Temporal succession and spatial heterogeneity in phytoplankton. In: Buzzati-Traverso A.A. (ed) *Perspective in marine biology*. University of California Press, Berkeley and Los Angeles, pp. 323-349

Marie D., Partensky, F., Simon, N., Guillou, L., Vaulot, D. (2000) Flow cytometry analysis of marine picoplankton. In: Diamond R.A. and DeMaggio, S. (eds) *In living colors: Protocols in flow cytometry and cell sorting*. Springer-Verlag, Berlin, pp. 421-454

Menden-Deuer S., Lessard, E.J. (2000) Carbon to volume relationships for dinoflagellates, diatoms, and other protist plankton. *Limnol Oceanogr,* **45**, 569-579

Moloney C.L., Field, J.G. (1989) Generic allometric equations for rates of nutrient uptake, ingestion, and respiration in plankton organisms. *Limnol Oceanogr,* **34**, 1290-1299

Moloney C.L., Field, J.G. (1991) The size-based dynamics of plankton food webs. I. A simulation model of carbon and nitrogen flows. *J Plankton Res,* **13**, 1003-1038

Moran X.A.G., Lopez-Urrutia, A., Calvo-Diaz, A., Li, W.K.W. (2010) Increasing importance of samll phytoplankton in a warmer ocean. *Global Change Biol,* **16**, 1137-1144

Pelegri S.P., Dolan, J.R., Rassoulzadegan, F. (1999) Use of high temperature catalytic oxidation (HTCO) to measure carbon content of microorganisms. *Aquat Microb Ecol,* **16**, 273-280

Peters R.H., Downing, J.A. (1984) Empirical Analysis of Zooplankton Filtering and Feeding Rates. *Limnol Oceanogr,* **29**, 763-784

Pierce R.W., Turner, J.T. (1992) Ecology of planktonic ciliates in marine food webs. *Rev Aquat S,* **6**, 139-181

Platt T., Denman, K.L. (1977) Organisation in the pelagic ecosystem. *Helgolander Meeresun,* **30**, 575-581

Putt M., Stoecker, D.K. (1989) An experimentally determined carbon: volume ratio for marine "oligotrichous" ciliates from estuarine and coastal waters. *Limnol Oceanogr,* **34**, 1097-1103

Rodriguez J., Mullin, M.M. (1986) Relation between biomass and body weight of plankton in a steady state oceanic ecosystem. *Limnol Oceanogr,* **31**, 361-370

Sanders R.W. (1987) Tintinnids and other microzooplankton - seasonal distributions and relationships to resources and hydrography in a Maine estuary. *J Plankton Res,* **9**, 65-77

Sautour B., Castel, J. (1998) Importance of microzooplanktonic crustaceans in the coastal food chain: Bay of Marennes-Oleron, France. *Oceanologica Acta,* **21**, 105-112

Sherr E., Sherr, B.F., Paffenhofer, G.-A. (1986) Phagotrophic protozoa as food for metazoans : a "missing" trophic link in marine pelagic food webs? *Mar Microb Food Webs,* **1**, 61-80

Sherr E.B., Caron, D.A., Sherr, B.F. (1994) Staining of heterotrophic protists for visualisation *via* epifluorescence microscopy. In: Kemp P.F., Sherr, B.F., Sherr, E.B. and Coll, J.J. (eds) *Handbook of methods in aquatic microbial ecology*. Lewis Publishers, Boca Raton, pp. 213-227

Sherr E.B., Sherr, B.F. (2000) Marine microbes: an overview. In: Kirchman D.L. (ed) *Microbial ecology of the oceans*. Wiley-Liss, New York, pp. 13-46

Shinada A., Ban, S., Ikeda, T. (2003) Seasonal changes in nano/micro-zooplankton herbivory and heterotrophic nano-flagellates bacterivory off Cape Esan, Southwestern Hokkaido, Japan. *J Oceanogr,* **59**, 609-618

Shinada A., Ban, S., Yamada, Y., Ikeda, T. (2005) Seasonal variations of plankton food web structure in the coastal water off Usujiri Southwestern Hokkaido, Japan. *J Oceanogr,* **61**, 645-654

Sieburth J.M., Smetacek, V., Lenz, J. (1978) Pelagic Ecosystem Structure: Heterotrophic Compartments of the Plankton and Their Relationship to Plankton Size Fractions. *Limnol Oceanogr,* **23**, 1256-1263

Sieracki C.K., Sieracki, M.E., Yentsch, C.S. (1998) An imaging-in-flow system for automated analysis of marine microplankton. *Mar Ecol Prog Ser,* **168**, 285-296

Sleigh M.A. (1991) A taxonomic review of heterotrophic protists important in marine ecology. In: Reid P.C., Turley, C.M. and Burkill, P.H. (eds) *Protozoa and their role in marine processes*. Springer-Verlag, Berlin, pp. 9-38

Sommaruga R. (1995) Microbial and classical food webs: A visit to a hypertrophic lake. *FEMS Microbiol Ecol,* **17**, 257-270

Stock C.A., Powell, T.M., Levin, S.A. (2008) Bottom-up and top-down forcing in a simple size-structured plankton dynamics model. *J Mar Syst,* **74**, 134-152

Strickland J.D.H., Parsons, T.R. (1972) A practical handbook of seawater analysis. *Bull Fish Res Board Can,* **167,** 47-89

Thingstad T.F., Rassoulzadegan, F. (1999) Conceptual models for the biogeochemical role of the photic zone microbial food web, with particular reference to the Mediterranean Sea. *Prog Oceanogr,* **44**, 271-286

Uitto A., Heiskanen, A.-S., Lignell, R., Autio, R., Pajuniemi, R. (1997) Summer dynamics of the coastal planktonic food web in the northern Baltic Sea. *Mar Ecol Prog Ser,* **151**, 27-41

Utermöhl H. (1958) Zur Vervollkommung der quantitativen phytoplankton-methodik. *Mitteilungen Internationale Vereiningung fur Theoretische und Angewandte Limnologie,* **9**, 1-38

Valiela I. (1995) *Marine ecological processes*, Springer-Verlag, New York

Verity P.G., Langdon, C. (1984) Relationships between Lorica volume, carbon, nitrogen, and ATP content of tintinnids in Narrangansett Bay. *J Plankton Res,* **6**, 859-868

Verity P.G. (1986) Growth rates of natural tintinnid populations in Narragansett Bay. *Mar Ecol Prog Ser,* **29**, 117-126

Waterbury J.B., Watson, S.W., Guillard, R.R.L., Brand, L.E. (1979) Widespread occurence of a unicellular, marine, planktonic, cyanobacterium. *Nature,* **277**, 293-294

West G.B., Savage, V.M., Gillooly, J., Enquist, B.J., Woodruff, W.H., Brown, J.H. (2003) Physiology (communication arising): Why does metabolic rate scale with body size? *Nature,* **421**, 713-713

Zeuthen E. (1970) Rate of living as related to body size of organisms. *Polskie Arch Hydrobiol,* **17**, 21-30

FIGURE CAPTIONS

Figure 1: Map of the Bay of Biscay with the location of the three study sites. Dashed line is a schematic representation of the continental shelf limits.

Figure 2: Variations of the Body Size (ngC) of nano-microzooplankton cells depending on their ESD (µm).

Figure 3: Temperature (°C) and salinity (PSU) profiles of the water column at the three stations and the four sampling periods.

Figure 4: Seasonal variations of nutrient concentration averages (µM) over the photic zone of the three stations: Nitrites and Nitrates (N tot), Phosphates (PO_4) and Silicates (Si).

Figure 5: Seasonal variations of the average autotrophic biomass (a) and its relative composition (b) over the photic zone at the three stations. Diat>20 for diatoms > 20µm, Diat<20 for diatoms < 20µm, ADF>20 for autotrophic dinoflagellates > 20µm, ADF<20 for autotrophic dinoflagellates < 20µm, ANF for autotrophic nanoflagellates, Picoeuk for eukaryotic picophytoplankton, Cyanobac for cyanobacteria.

Figure 6: Seasonal variations of average biomass of nano-microzooplankton (a) and its relative composition (b) over the photic zone at the three stations. HNF for Heteronanoflagellates; U-HDF for Unarmoured Hetero-dinoflagellates; A-HDF for Armoured Hetero-dinoflagellates; N-Cil for Naked Ciliates; Tint for Tintinnid Ciliates; Mr-Cil for Myrionecta rubra ciliates; Meta for Metazoans.

Figure 7: Size-abundance spectra and corresponding fitted linear regression (r^2>0.7) of nano-microzooplankton at the 3 sites and for the 4 sampling periods. Size is represented by cell biovolumes (μm^3).

Figure 8: Temporal and spatial variations of the linear regression slope of the size-abundance spectra as presented in figure 6.

Figure 9: Seasonal variations of the nano-microzooplankton community structure over the photic zone at the three stations in terms of relative biomasses of (a) ESD size (µm) classes and (b) body size (ngC $cell^{-1}$) classes.

TABLE CAPTIONS

Table 1: Factors and formulae with their reference used to convert biovolume to carbon mass of each plankton organisms.

Table 2: Seasonal abundances (cells l^{-1}) with their standard deviations, of the different nano-microzooplankton classes from the 3 classification types (Taxons, ESD and Body Size) in average over the photic zone at the three stations.

Table 3: Statistical details of the Mantel tests run to compare similarities between the dynamics of nano-microzooplankton community using three different classification types: Taxons, Body Size and ESD. r refers to Pearson correlation coefficient. Statistical significance (p) was estimated using 10,000 permutations.

Table 4. Statistical details of the BEST analysis run to link nano-microzooplankton dynamics and environmental conditions (biological and physical conditions). r refers to Spearman rank correlation coefficient. Statistical significance (p) was estimated with permutations and is < 0.01.

Table 1

Plankton organisms	*Conversion factor or formulae*	*References*
Bacteria	0.016 pgC $cell^{-1}$	Labry et al. (2002)
Cyanobacteria	0.104 pgC $cell^{-1}$	Blanchot and Rodier (1996)
Eucaryotic picophytoplankton	0.22 pgC $cell^{-1}$	Shinada et al. (2005)
Nanoflagellates	0.125 pgC μm^{-3} = 3.14 pgC $cell^{-1}$ (with mean biovolume of 25.2 μm^3)	Pelegri et al. (1999) and our data of biovolumes
Dinoflagellates	Log_{10} C (in pgC $cell^{-1}$) = -0.353 + 0.864 * log_{10} V	Menden-Deuer & Lessard (2000)
Diatoms	Log_{10} C (in pgC $cell^{-1}$) = -0.541 + 0.811 * log_{10} V Log_{10} C (in pgC $cell^{-1}$) = -0.933 + 0.881 * log_{10} V	< 3000 μm^3 > 3000 μm^3 Menden-Deuer & Lessard (2000)
Naked Ciliates	0.19 pgC μm^{-3}	Putt & Stoecker (1989)
Ciliate Tintinnids	C (in pgC $cell^{-1}$) = 444.5 + 0.053 * LV	Verity & Langdon (1984)
Copepod Nauplii	pgC ind^{-3} = 0.08 × V	Gowing et al. (2003)

V: biovolume (in μm^3) and LV: Lorica volume (in μm^3)

Table 2

Classification	Class	Gironde				Coast				Offshore			
		February	April	June	October	February	April	June	October	February	April	June	October
Taxons	**HNF** (10^4)	12.7 ± 1.9	5.5 ± 2.6	4.4 ± 4.2	16.2 ± 14.2	14.6 ± 8.5	3.0 ± 0.8	1.7 ± 0.9	2.5 ± 2.4	15.4 ± 4.2	1.2 ± 1.0	1.0 ± 1.7	0.6 ± 0.6
	Mr-Cil	0.0 ± 0.0	543.4 ± 413.3	64.6 ± 47.5	0.0 ± 0.0	68.4 ± 118.5	2810.1 ± 2517.3	55.1 ± 64.1	11.4 ± 19.7	108.3 ± 114.4	963.3 ± 1123.6	3.8 ± 6.6	19.0 ± 11.9
	Nak-Cil	53.2 ± 92.1	4115.4 ± 2161.6	2976.4 ± 4479.3	596.6 ± 638.2	1411.4 ± 1272.4	6627.2 ± 4211.9	3345.9 ± 4582.3	471.2 ± 668.7	2471.9 ± 1587.9	2346.5 ± 1482.4	463.6 ± 125.1	469.8 ± 387.8
	Tint	7.6 ± 13.2	7.6 ± 13.2	9.5 ± 8.7	38.0 ± 8.7	318.6 ± 503.3	0.0 ± 0.0	17.1 ± 17.1	22.8 ± 26.1	19.0 ± 3.3	1.9 ± 3.3	0.0 ± 0.0	0.0 ± 0.0
	U-HDF	1040.0 ± 750.0	18373.3 ± 13130.9	5985.8 ± 10188.1	332.0 ± 394.8	277.3 ± 317.7	12133.3 ± 8002.8	8437.9 ± 7677.3	1061.9 ± 961.3	7522.7 ± 2422.0	11856.0 ± 4632.4	5477.3 ± 4993.4	2617.3 ± 2858.7
	A-HDF	485.3 ± 240.1	1109.3 ± 1067.4	2357.3 ± 2582.1	100.8 ± 104.1	69.3 ± 120.1	485.3 ± 317.7	1079.3 ± 237.8	434.7 ± 344.9	520.0 ± 375.0	485.3 ± 120.1	225.3 ± 346.2	28.9 ± 26.5
	Meta	43.1 ± 23.0	44.3 ± 4.5	31.2 ± 16.9	47.6 ± 28.9	20.4 ± 26.5	39.6 ± 5.5	17.5 ± 28.2	24.3 ± 23.8	30.2 ± 13.0	12.4 ± 7.0	12.1 ± 10.9	2.5 ± 2.3
ESD (µm)	**<20** (10^4)	12.7 ± 1.9	5.5 ± 2.6	4.4 ± 4.2	16.2 ± 14.2	14.6 ± 8.5	3.0 ± 0.8	1.7 ± 0.9	2.5 ± 2.4	15.4 ± 4.2	1.2 ± 1.0	1.0 ± 1.7	0.6 ± 0.6
	20-30	208.0 ± 360.3	383.8 ± 399.9	340.1 ± 564.5	19.0 ± 18.3	269.8 ± 373.0	442.7 ± 327.5	1448.2 ± 2258.4	140.6 ± 204.4	1025.0 ± 895.8	231.8 ± 171.0	382.8 ± 337.7	85.0 ± 68.8
	30-40	208.0 ± 360.3	10931.1 ± 5560.6	695.3 ± 997.4	224.4 ± 378.9	387.7 ± 102.6	9717.9 ± 8463.8	3493.3 ± 1988.0	963.4 ± 1003.0	6377.8 ± 2750.1	7481.7 ± 656.5	2711.1 ± 2199.8	1474.3 ± 1674.2
	40-50	962.1 ± 621.5	10743.6 ± 7571.3	9746.1 ± 14674.9	691.0 ± 637.4	1281.4 ± 252.7	9044.8 ± 4960.9	7146.6 ± 3614.6	840.8 ± 484.7	2707.1 ± 1143.9	6872.9 ± 4255.0	2899.5 ± 2591.3	1442.9 1271.6
	50-60	208.0 ± 208.0	1980.3 ± 1230.6	554.1 ± 910.4	123.5 ± 3.3	96.0 ± 55.2	2018.4 ± 919.2	702.9 ± 1052.2	53.4 ± 31.8	492.0 ± 581.7	872.9 ± 1014.4	150.1 ± 230.4	118.8 89.1
	60-70	0.0 ± 0.0	110.2 ± 133.6	38.0 ± 3.3	9.5 ± 8.7	110.2 ± 162.2	826.5 ± 1180.0	144.4 ± 86.3	3.8 ± 6.6	39.9 ± 64.2	193.8 ± 243.7	26.6 ± 46.1	14.1 ± 19.7
	>70	43.1 ± 23.0	44.3 ± 4.5	31.2 ± 16.9	47.6 ± 28.9	20.4 ± 26.5	45.3 ± 13.9	17.5 ± 28.2	24.3 ± 23.8	30.2 ± 13.0	12.4 ± 7.0	12.1 ± 10.9	2.5 ± 2.3
Body Size (ngC cell^{-1})	**<0.1** (10^4)	12.7 ± 1.9	5.5 ± 2.6	4.4 ± 4.2	16.2 ± 14.2	14.6 ± 8.5	3.0 ± 0.8	1.7 ± 0.9	2.5 ± 2.4	15.4 ± 4.2	1.2 ± 1.0	1.0 ± 1.7	0.6 ± 0.6
	0.1-1	416.0 ± 360.3	15097.9 ± 8258.5	2192.3 ± 3322.6	399.7 ± 561.0	974.8 ± 611.8	11454.2 ± 8610.1	6147.3 ± 3526.5	1104.0 ± 1200.4	7988.9 ± 1661.2	8365.0 ± 1406.7	3472.7 ± 1756.3	1678.7 ± 1775.2
	1-5	823.5 ± 403.3	8784.2 ± 5577.8	8864.0 ± 13389.0	576.5 ± 467.7	1045.8 ± 54.7	8374.2 ± 4850.9	6565.7 ± 3039.4	861.7 ± 496.9	2524.7 ± 1272.0	6414.1 ± 3654.4	2524.5 ± 2768.0	1323.3 ± 1199.6
	5-10	138.7 ± 240.7	152.9 ± 74.3	279.3 ± 439.3	72.2 ± 6.6	7.6 ± 13.2	1299.4 ± 821.6	77.9 ± 120.4	30.6 ± 43.6	84.5 ± 126.7	670.6 ± 1000.0	146.3 ± 233.9	107.4 ± 93.2
	10-50	208.0 ± 360.3	68.4 ± 71.2	38.0 ± 3.3	19.0 ± 11.9	116.9 ± 155.6	911.0 ±1306.5	142.5 ± 89.6	1.9 ± 3.3	43.7 ± 70.8	85.5 ± 70.0	0.0 ± 0.0	11.6 ± 20.0
	50-100	43.1 ± 23.0	89.9 ± 58.4	31.2 ± 16.9	47.6 ± 28.9	20.4 ± 26.5	51.0 ± 22.4	19.4 ± 26.7	28.1 ± 30.2	30.2 ± 13.0	130.2 ± 210.9	38.7 ± 35.7	16.6 ± 22.0
	>100	0.0 ± 0.0	0.0 ± 0.0	0.0 ± 0.0	0.0 ± 0.0	0.0 ± 0.0	5.7 ± 9.9	0.0 ± 0.0	0.0 ± 0.0	0.0 ± 0.0	0.0 ± 0.0	0.0 ± 0.0	0.0 ± 0.0

Table 3

Explanatory datasets	Mantel statistics	
	r	p
Taxons vs. Body Size	0.890	0.0001
Taxons vs. ESD	0.902	0.0001
Body Size vs. ESD	0.910	0.0001

Table 4.

Environmental conditions	Best parameters	Correlation coefficient r		
		Taxon classification	*ESD classification*	*Body Size classification*
Physical	Temperature and NO3 concentration	0.451	0.436	0.430
Biological	Bacteria and Cyanobacteria biomasses			0.307
	Bacteria, Cyanobacteria and ANF biomasses	0.326	0.308	

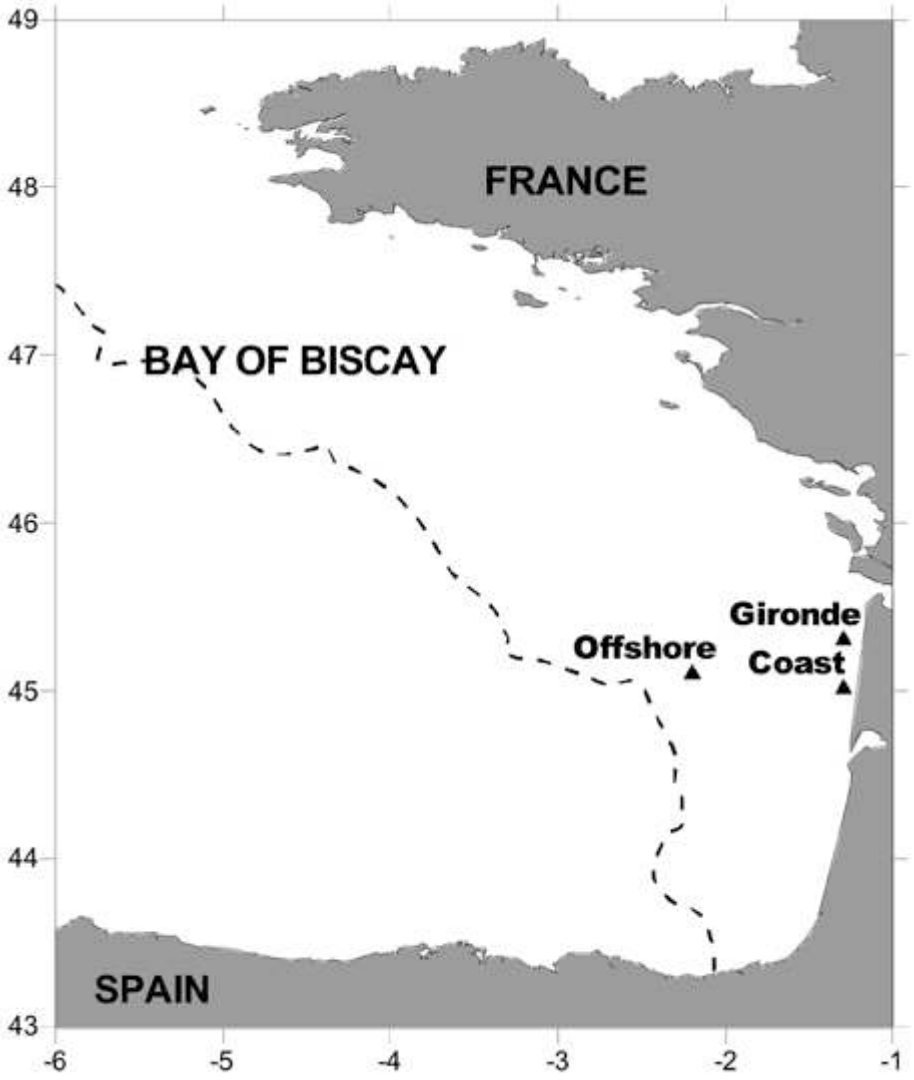

Figure 1
172x201mm (72 x 72 DPI)

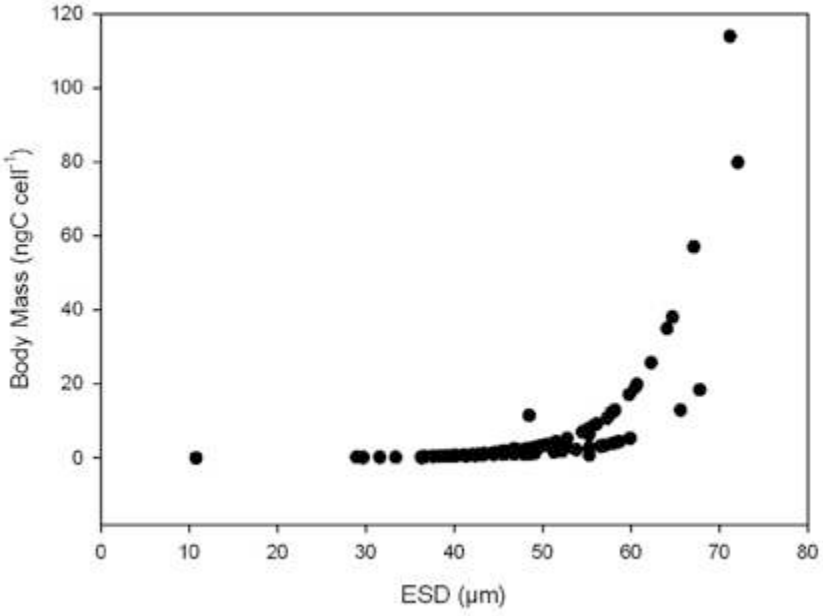

Figure 2
163x119mm (72 x 72 DPI)

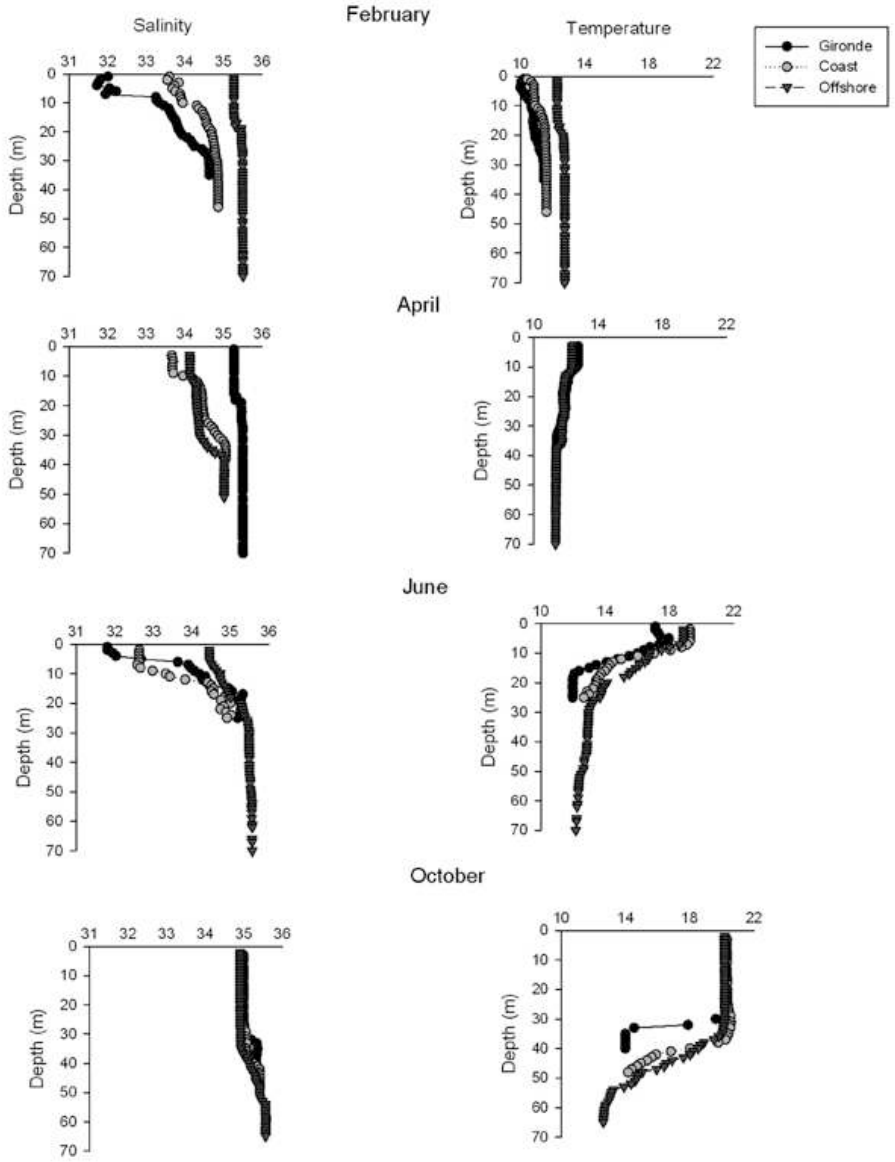

Figure 3
215x279mm (72 x 72 DPI)

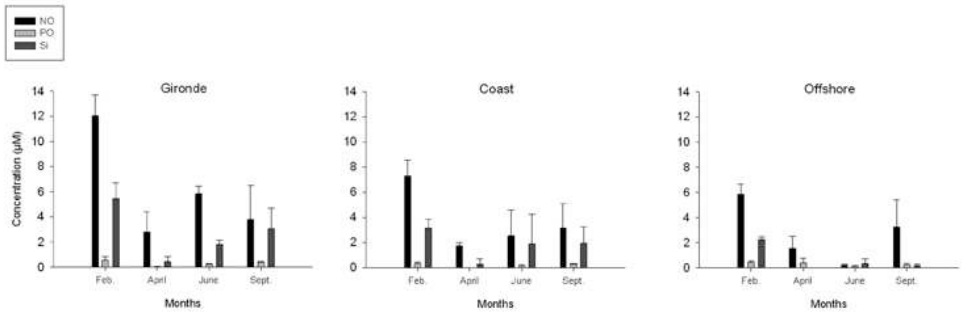

Figure 4
268x90mm (72 x 72 DPI)

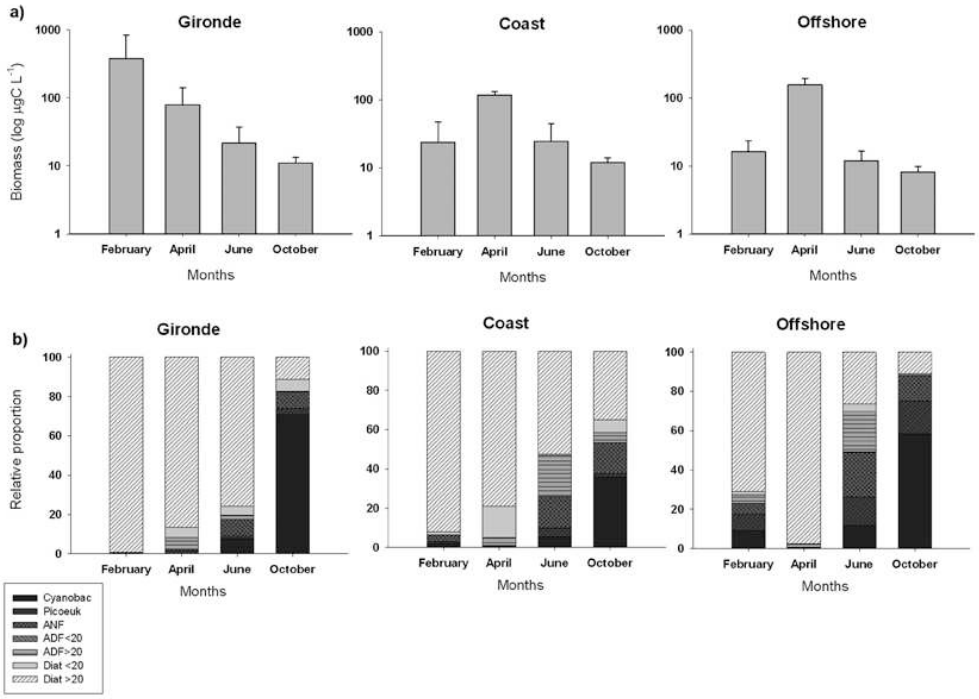

Figure 5
296x210mm (72 x 72 DPI)

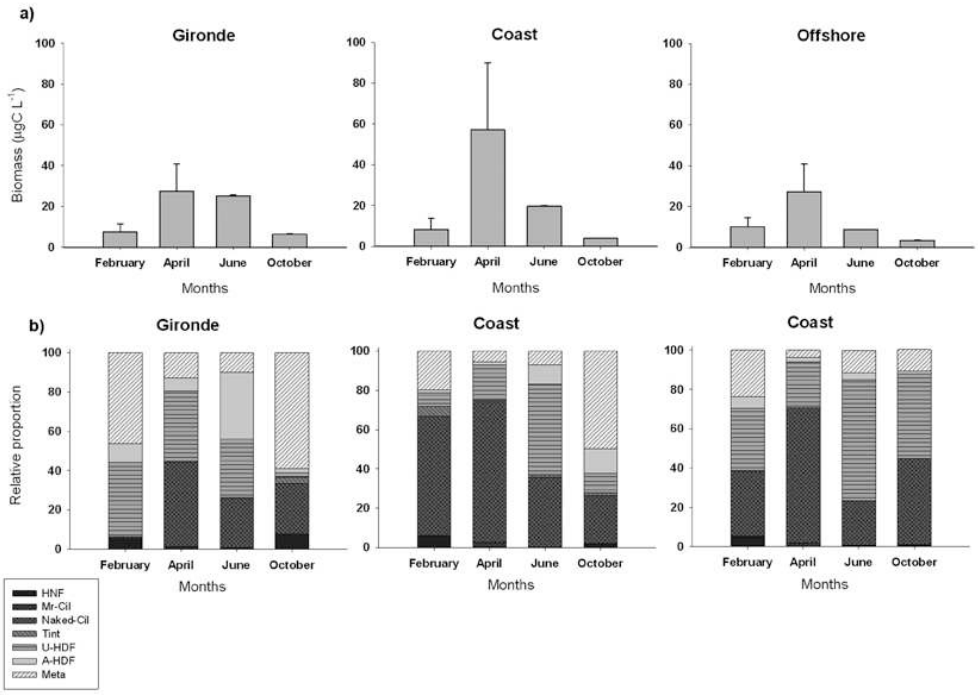

Figure 6
296x210mm (72 x 72 DPI)

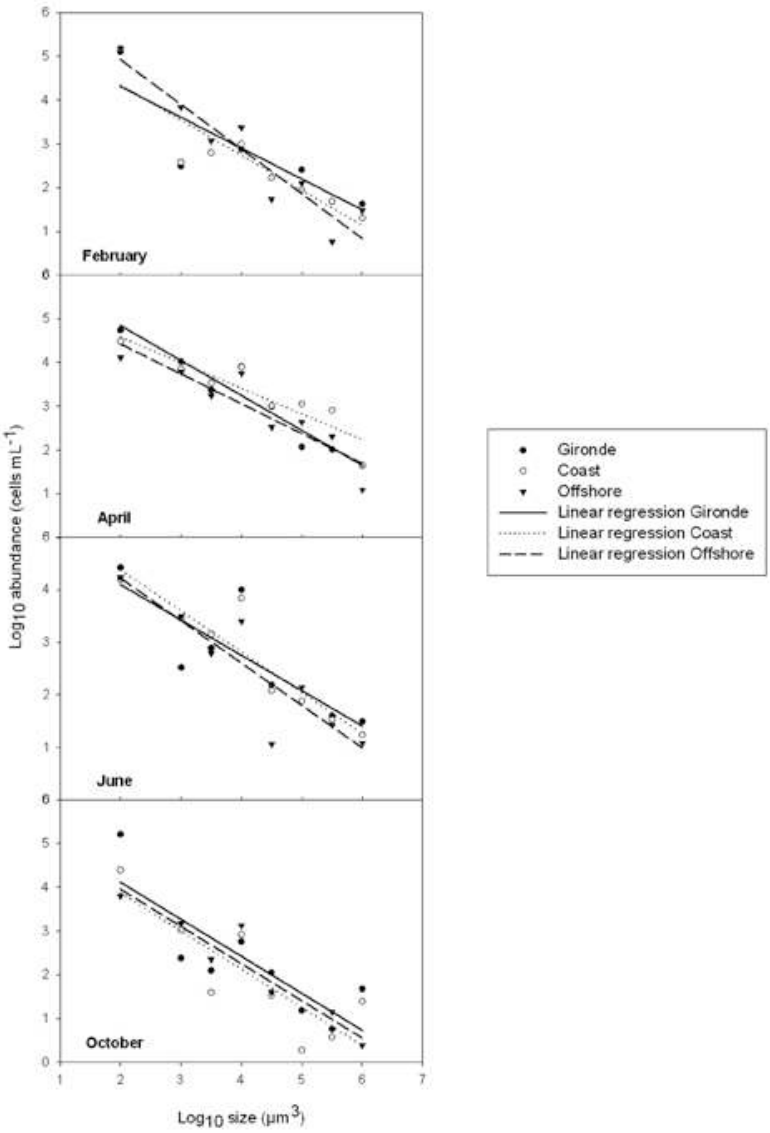

Figure 7
173x254mm (72 x 72 DPI)

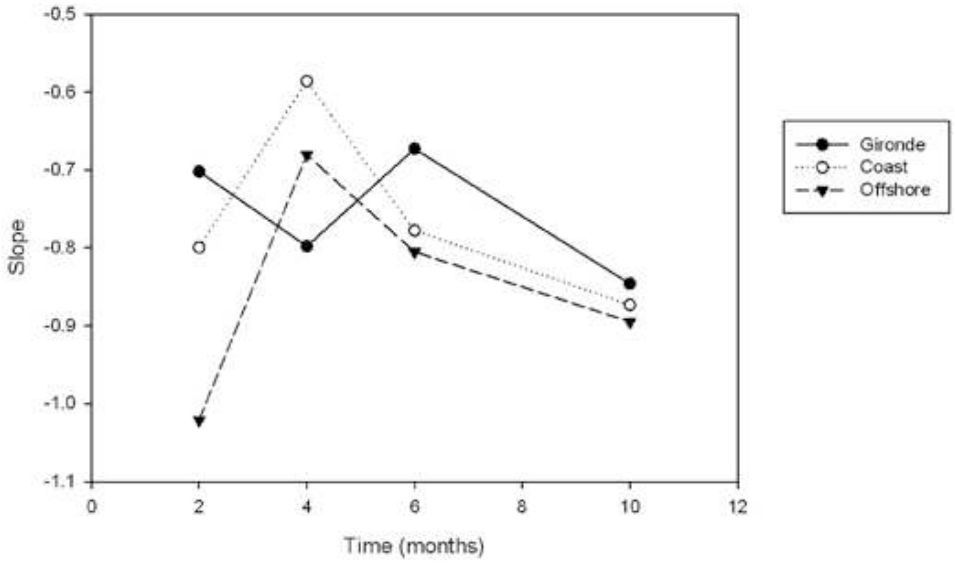

Figure 8
192x127mm (72 x 72 DPI)

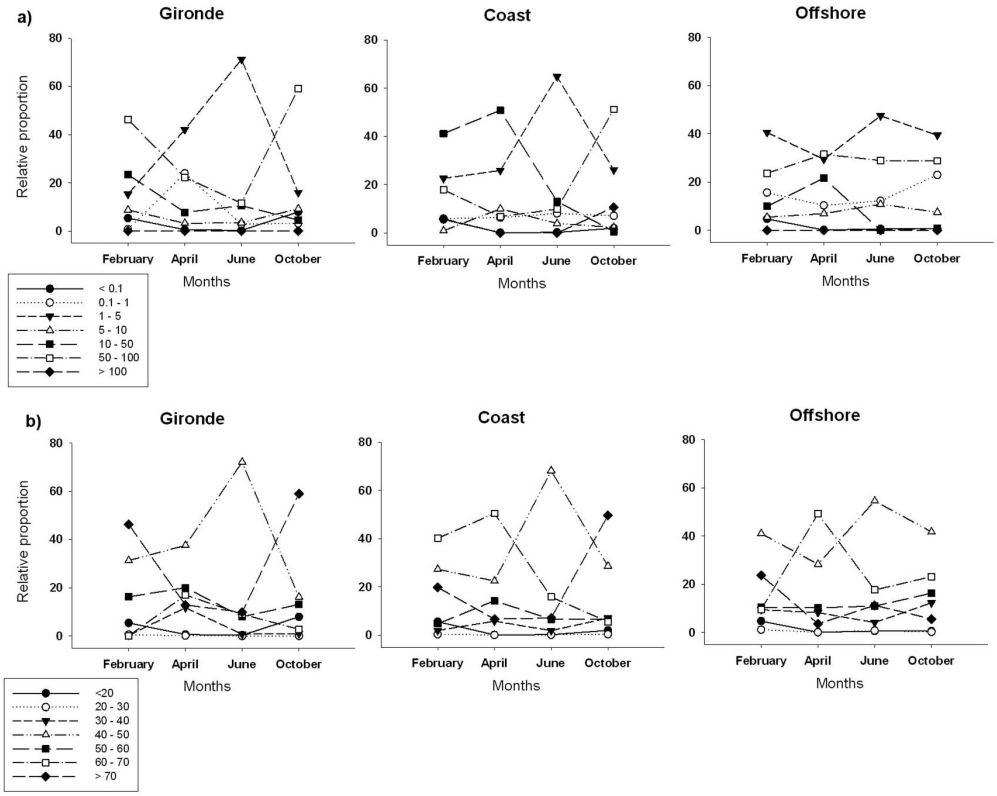

Figure 9
289x231mm (300 x 300 DPI)